Co_3O_4 ethylene glycol-based nanofluids: Thermal conductivity, viscosity and high pressure density

Alejandra Mariano [a,*,1], María José Pastoriza-Gallego [b], Luis Lugo [b], Lelia Mussari [a], Manuel M. Piñeiro [b]

[a] Facultad de Ingeniería, Universidad Nacional del Comahue, Neuquén 8300, Argentina
[b] Departamento de Física Aplicada, Facultade de Ciencias, Universidade de Vigo, E-36310 Vigo, Spain

A B S T R A C T

This work contributes with experimental information of the properties of ethylene glycol-based Co_3O_4 nanofluids. Thermal conductivity, high-pressure density and rheological characterization were performed in the temperature range $T = (283.15–323.15)$ K. Thermal conductivity and rheological behaviour were studied for nanofluid samples with concentrations of Co_3O_4 nanoparticles up to 25% in weight fraction whereas the densities of the nanofluid were analysed up to 5% at pressures up to 45 MPa. Thermal conductivity showed in the range studied an increase with weight fraction and a decrease with temperature. A volumetric contractive behaviour was observed, and an increment in the nanoparticles concentration leads to a clear departure from ideal behaviour. The tests performed to analyse rheological properties showed that the viscosity of the nanofluids is nearly independent of the shear rate, thus evidencing the characteristic behaviour of a Newtonian fluid. Experimental viscosity and thermal conductivity were also compared with the estimations provided by several semiempirical equations proposed in the literature.

© 2015 Elsevier Ltd. All rights reserved.

1. Introduction

The suspension of nanoscale particles in a fluid is a colloidal system usually denoted as nanofluid, and their study is an active research field nowadays because the effects of the nanometric sized particles on the suspension thermophysical and transport properties show unusual trends. The atypical increases in properties such as thermal conductivity or viscosity is related with the system scale, determined by the size, nature, and state of aggregation of the particles in suspension, among other variables, and do not depend only on its chemical nature. This behaviour has been reported in literature for nanofluids derived from metallic nanoparticles, nanoparticles derived from metal oxides, ceramics, or carbon nanotubes [1–9].

In a recently published work [10], the authors made a extensive compilation of articles reporting thermal conductivity of different nanofluids, pointing out that their thermal conductivity depends on factors like volume fraction, nanoparticle size, morphology, additives, pH, temperature, nature of base fluid, nanoparticle material, etc. This represents a major concern related with sample char-

acterization and experimental data reproducibility, and a literature revision reveals that there are important discrepancies between different thermal conductivity data sets reported for this type of systems. It is generally agreed that the combination of factors as the diversity of preparation processes, samples stability, particle size dispersion, non-uniformity of the particle shape, clustering, sedimentation or pH are related with those discrepancies [10–13]. Regarding transport properties, including viscosity and other viscoelastic properties, nanofluids also exhibit unusual behaviour [1,14–21] and this represents a challenge, not only for to the difficulties associated to their experimental determination, but also for the very limited knowledge about the underlying physicochemical phenomena that might justify the observed trends.

One of the possible industrial applications of nanofluids is the industry of refrigerants and lubricating oils in refrigeration systems. In a recent review [22] the authors suggest that experimental results of specific heat, density, and viscosity of nanofluids are scarce in literature, highlighting the importance of creating reliable and wide experimental databases.

Several experimental studies about magnetic and electric properties of dry Co_3O_4 nanoparticles have been published in the last years [23–26], but only a few works published recently [27,28] studied the properties of Co_3O_4 nanoparticles dispersed in a fluid. Vickers et al. [27] reported rheological properties of suspensions

of Co$_3$O$_4$ nanocubes in oligomeric polyethylene glycol (PEG) at 323.15 K, over a wide range of particle volume fractions and rotational shear flow conditions, finding that at low volume fractions the suspensions studied behaved as Newtonian liquids whereas at intermediate to high particle volume fraction the suspensions showed complex rheological behaviour, including shear thinning and shear-thickening features. Hosseini et al. [28] studied the effect of nanoparticle concentration on the rheological properties of Co$_3$O$_4$ nanoparticle dispersed in paraffin, using oleic acid as nanoparticle capping agent, pointing out non-Newtonian behaviour for all samples.

The objective of this article is to study nanofluids composed by Co$_3$O$_4$ nanoparticles dispersed in ethylene glycol (EG), in a concentration up to 25% in weight fraction. The research includes the dry powder characteristics, size distribution and suspension stability; measurements of thermal conductivity applying the hot-wire technique; rheological analyses using a Physica MCR 101 Rheometer (Anton Paar, Austria) and high-pressure densities measurements using an Anton Paar DMA 512P vibrating tube densimeter. The effects of both volume fraction and temperature were evaluated for the different properties studied, and the experimental values were compared with theoretical models.

2. Experimental

2.1. Sample preparation and characterization

The Co$_3$O$_4$ nanofluid samples used in this work were prepared from cobalt(II, III) oxide nanopowder provided by Aldrich, with a declared diameter distribution $D < 50$ nm. Ethylene glycol, used as base fluid, was supplied also by Aldrich (99%). The nanofluids samples were prepared weighting the nanoparticle powder with a Mettler AE-240 electronic balance, whose uncertainty is, according to the manufacturer specifications, $5 \cdot 10^{-5}$ g. The powder was dispersed into a volume of the base fluid to obtain the desired weight percentage. The estimated uncertainty on weight fraction was lower than 0.03%.

The size and morphology of the Co$_3$O$_2$ nanoparticles in EG (0.005% v/v) were studied using the technique of transmission electron microscopy (TEM). The equipment used was a JEOL JEM-101 FEG (100 kV) microscope. The TEM image of the Co$_3$O$_4$ nanoparticles is shown in Fig. 1. The size distribution of Co$_3$O$_4$ nanoparticles was computed by measuring the size of a large number of nanoparticles on a set of TEM images, and it is shown in Fig. 2, evidencing lognormal distribution, and average diameter of $D = (17 \pm 7)$ nm.
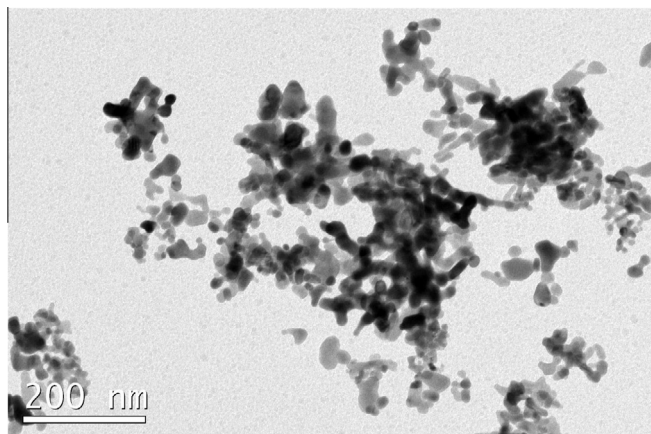

Fig. 1. TEM images of Co$_3$O$_4$ (JEOL JEM-101 FEG (100 kV) microscope) nanoparticles in ethylene glycol, at a concentration of 0.005% v/v.
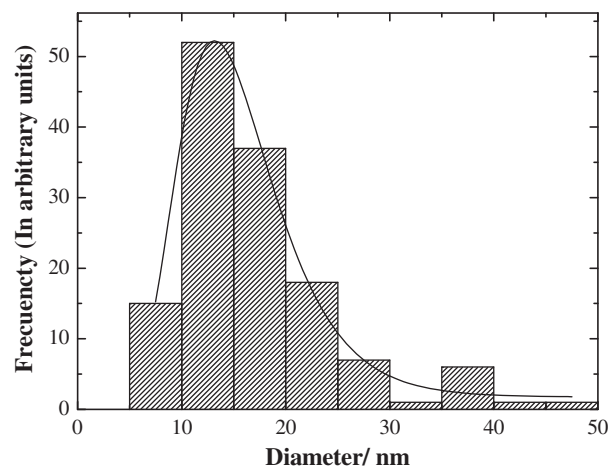

Fig. 2. Size distribution of Co$_3$O$_4$ nanoparticles in ethylene glycol, at a concentration of 0.005% v/v.

A spectrometer Agilent HP 8453 UV–Vis equipped with a thermostated cell carrier was used to evaluate the stability of the nanofluid, and a typical recording for the optical absorption spectrum of Co$_3$O$_4$/EG nanofluid is shown in Fig. 3. The absorbance time evolution for the sample was analysed at two wavelength values close to the maxima, $\lambda = 205$ nm and $\lambda = 410$ nm. The results obtained in each case, indicate that the absorbance decrease is lower than 1% in 24 h, so the sample is stable for the type of measurements performed in this work, given that the time employed in sample dispersion was very short. Nanofluid samples were prepared using an Ultrasonic homogenizer probe (Bandelin Sonopuls 2200HD). More details about the different sonication methods were discussed in a previous work [4].

2.2. Measurements

Once the samples were characterised, thermal conductivity, rheological behaviour and high-pressure density of Co$_3$O$_2$ nanofluids were measured. Thermal conductivity was measured using a Decagon Devices KD2 Pro Thermal Properties Analyser (Decagon Devices Inc., Pullman, WA, USA), whose principle of measurement is based on the transient hot-wire method, pointed out by several authors [11,13] as one of the most accurate methods to determine nanofluids thermal conductivity. Heating the probe immersed in the sample and simultaneously monitoring its temperature evolution allows to calculate the fluid thermal conductivity, in agreement with the model proposed by Carslaw and Jaeger [29]. The estimated uncertainty of thermal conductivity measurement was
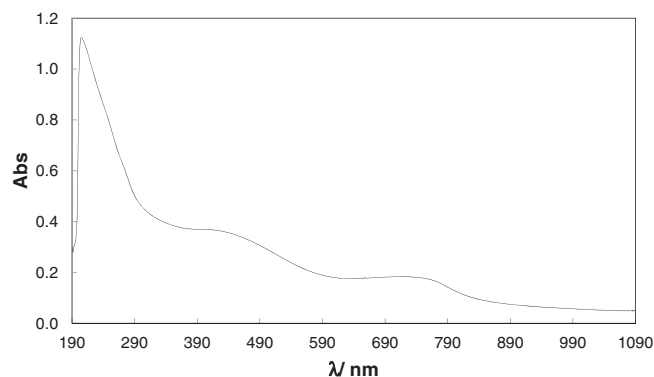

Fig. 3. UV–Vis absorption spectrum of Co$_3$O$_4$/EG nanofluid, 0.01% wt, $T = 298.15$ K.

lower than 3%. In previous works [30–32] the advantages of this technique applied to nanofluids has been discussed.

The rheological behaviour of the Co_3O_4 nanofluids was analysed using a Physica MCR 101 rheometer (Anton Paar, Austria). This equipment, as pointed out in previous papers [20,33], allows to control torques between 0.1 μN m and 125 mN m, and normal forces between 0.1 and 30 N. A cone-plate geometry was used, with a cone diameter and angle of 25 mm and 1°, respectively. All nanofluid samples were analysed at a constant gap value of 0.048 mm and temperature was controlled using a Peltier system. Non-linear viscoelastic experiments, usually referred to as flow curves, where shear viscosity variation with shear rate is measured, were performed for Co_3O_4 nanofluids samples.

High-pressure densities were measured with an Anton Paar DMA 512P vibrating tube densimeter. The experimental procedure, calibration, temperature and pressure control were detailed in previous works [34,35]. The uncertainty on high pressure density was estimated from the uncertainties of the reference substances used for calibration, water and vacuum in this case, according with the procedure introduced by Lagourette et al. [36], and was estimated to be lower than 10^{-4} g cm^{-3}.

3. Results and discussion

3.1. Thermal conductivity

Thermal conductivity of four different Co_3O_4/EG nanofluids samples were measured at 283.15 K, 303.15 K and 323.15 K, and experimental data, κ_{nf}, are shown in Table 1 as a function of volume fraction, ϕ. Volume fractions were estimated using the densities of the pure base fluid, ethylene glycol (1.0176 g/cm^3 at 303.15 K [30]) and the bulk solid oxide density (6.11 g/cm^3, value provided by the vendor). From Fig. 4(a) it can be noted that the addition of cobalt(II, III) oxide nanopowder increases thermal conductivity of the nanofluids for most samples studied, if compared with the base fluid. Average enhancement (κ_{nf}/κ_0, where the subscripts nf and 0 refer to the nanofluid and base fluid, respectively) values reach 27% for the highest concentration.

Over the temperature range of 283.15–323.15 K the thermal conductivity of the nanofluid, κ_{nf}, decreases very slightly with the increase in temperature as shown in Fig. 4. A similar trend κ_{nf} decrease with the increase in temperature was observed previously by other authors [37–40].

From a modelling perspective, Maxwell [41] was the first to propose an equation to estimate the thermal conductivity of colloids composed by solid spherical particles suspended in a fluid, as follows:

$$\kappa_{nf} = \frac{\kappa_p + 2\kappa_0 + 2(\kappa_p - \kappa_0)\phi}{\kappa_p + 2\kappa_0 - (\kappa_p - \kappa_0)\phi}\kappa_0 \tag{1}$$

where κ_{nf}, κ_p and κ_0 represent the thermal conductivity of the colloid, suspended solid particles, and base fluid, respectively, and ϕ is the percent volume concentration of solid particles. This expression

Table 1
Experimental values of thermal conductivity for Co_3O_4/EG nanofluids.

ϕ	κ (W m^{-1} K^{-1})		
	283.15 K	303.15 K	323.15 K
0.0000	0.243	0.246	0.249
0.0094	0.263	0.261	0.259
0.0206	0.274	0.273	0.271
0.0307	0.286	0.284	0.283
0.0431	0.297	0.296	0.294
0.0567	0.309	0.307	0.306
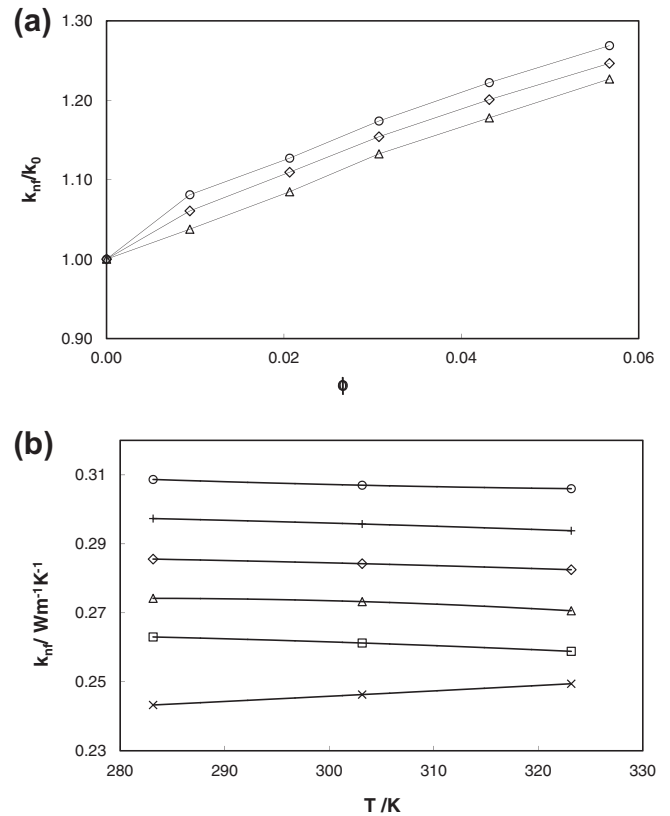
Fig. 4. (a) Enhancement in the thermal conductivity (κ_{nf}/κ_0) at (○) 283.15 K, (◇) 303.15 K and (△) 323.15 K of Co_3O_4/EG nanofluids as a function of nanoparticle volume fraction. (b) Thermal conductivity (κ_{nf}) as a function of temperature for different volume fractions of Co_3O_4/EG nanofluids: (×), $\phi = 0$; (□), $\phi = 0.0094$; (△), $\phi = 0.0206$; (◇), $\phi = 0.0310$; (+), $\phi = 0.0431$ and (○), $\phi = 0.0567$.

was later modified by Hamilton and Crosser (HC model) [42] taking into consideration the particle shape, and their model has been used for the description of the thermal conductivity enhancement of dilute suspensions of different shape particles in a liquid or a solid:

$$\frac{\kappa_{nf}}{\kappa_0} = \frac{\kappa_p + (n-1)\kappa_0 + (n-1)(\kappa_p - \kappa_0)\phi}{\kappa_p + (n-1)\kappa_0 - (\kappa_p - \kappa_0)\phi} \tag{2}$$

In this expression, n stands for the empirical shape factor, determined as $n = 3/\Psi$, where Ψ is the sphericity, calculated as the ratio of the surface of an hypothetical sphere which would have the same volume of the particle, divided by the real particle surface area. Turian et al. [43] evaluated a number of models using thermal conductivity data on many dispersions, concluding that the Maxwell model gives accurate estimations of thermal conductivity enhancements for dispersions when $\kappa_p/\kappa_0 \sim 1$, but its performance worsens as this ratio increases. For dispersions where $\kappa_p/\kappa_0 > 4$, the authors concluded that a volume averaged geometric mean of the thermal conductivities of both particle and base fluid yields the best estimates of the effective thermal conductivity. Logarithmic mixing rules have been used successfully to describe several properties of materials comprising inclusions embedded or dispersed in a medium [44]. Such mixing rules treat the properties of inclusions and matrix separately to obtain the effective property of the composite:

$$\kappa_{nf} = \kappa_p^\phi \kappa_0^{1-\phi} \tag{3}$$

Concerning the reference value for the thermal conductivity of the nanoparticles at T = 300 K, the value κ_p = 16.8 W m^{-1} K^{-1} has been used according to reference [45]. Experimental thermal

conductivity values at 303.15 K were then compared with the cited Maxwell, Hamilton and Crosser, and Turian estimations, and results are shown in Fig. 5. The obtained estimations evidence weak temperature dependence. As shown, the Maxwell model under predicts the experimental property enhancement at this temperature. The Turian model and HC-model yield good agreement with experimental data, and HC-model gives the best estimations when $\Psi = 0.61$. This numerical value has been fitted to the measured experimental data. The absolute average percent deviations of the experimental thermal conductivity with Maxwell, Turian and HC models are 4.3%, 1.4% and 1.4%, respectively.

3.2. Rheological behaviour

Fig. 6 shows the viscosity of pure ethylene glycol (EG) as a function of shear rate in the range 50–1000 s^{-1} at 303.15 K. The flow curves with particle weight concentrations of 5%, 10%, 15%, 20% and 25% were measured from 283.15 to 323.15 K at 10 K steps, and part of the results obtained at 303.15 K are plotted in Fig. 6. As shown, shear viscosity is independent of shear rate for pure EG and for nanofluids samples, evidencing Newtonian behaviour. The same behaviour was obtained at particle weight concentrations of 10% and 20%, and at temperatures from 283.15 to 323.15 K.

Shear viscosity for all concentrations and temperatures are shown in Fig. 7, pointing out that shear viscosity increases with particle weight concentrations and decreases with temperature, as expected.

The viscosity temperature dependence of a fluid can be correlated using the three-coefficient Vogel–Fulcher–Tammann (VFT) expression:

$$\text{Ln} (\eta) = A + \frac{B}{T - T_0} \tag{4}$$

where A, B and T_0 are the fitting coefficients. The ratio $B/2_0$ is denoted as Angell strength coefficient [46]. The fitted values for these coefficients are listed in Table 2, together with the average standard deviations. Fig. 7 shows the accuracy of this correlation.

As expected, viscosity increases with particle concentration, and this enhancement, defined as the ratio η_{nf}/η_0, where η_0 is the viscosity of the base fluid, and can be considered temperature dependent. Average viscosity increase for each sample at 303.15 K is shown in Fig. 8. For the experimental data presented here, at 5.7% volume fraction concentration viscosity enhancement of 40% is obtained.

These anomalous nanofluid experimental viscosity trends have been reported previously, the possible reasons that might explain
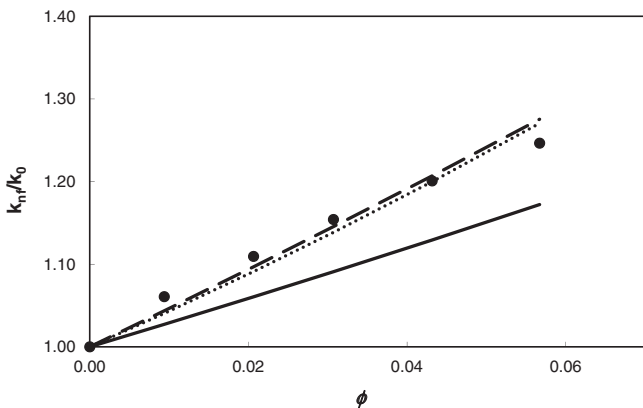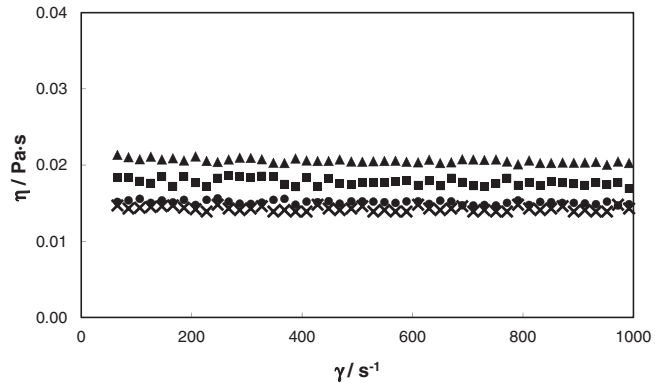
Fig. 6. Viscosity (η) versus shear rate ($\dot{\gamma}$) dependence of Co$_3$O$_4$/EG nanofluids at 303.15 K for different weight concentrations: ($\times$) EG; ($\bullet$) 5 wt%; ($\blacksquare$) 15 wt%; ($\blacktriangle$) 25 wt%.

Fig. 7. Dynamic viscosity (η) vs. T for EG/Co$_3$O$_4$ nanofluids at different volume fractions: ($\bullet$) EG; ($\circ$) 0.009; ($\blacklozenge$) 0.021; ($\lozenge$) 0.031; ($\blacksquare$) 0.043; ($\square$) 0.057. (—) Vogel–Fulcher–Tammann equation.
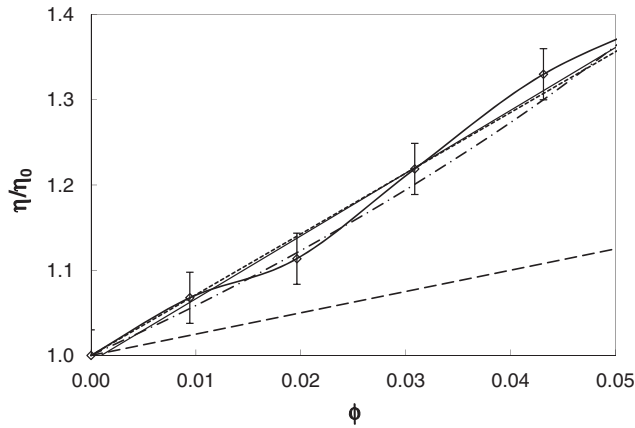
Table 2
Coefficients A, B, T_0 and standard deviation, s, from Vogel–Fulcher–Tammann equation for commercial Co$_3$O$_4$/EG nanofluids at different volume concentration, ϕ.

	ϕ					
	0.000	0.009	0.021	0.031	0.043	0.057
A	−3.51	−3.27	−3.87	−5.42	−2.93	−4.78
B (K)	998.5	998.4	1233.7	1917.4	997.7	1692.1
T_0 (K)	141.0	136.6	117.2	71.7	146.2	86.0
s (mPa s)	0.13	0.26	0.12	0.26	0.04	0.15

it remain controversial. Over the years a large number of semiempirical equations have been proposed to correlate this enhancement, ($\eta_r = \eta_{nf}/\eta_0$), where η_{nf} and η_0 are the nanofluid and base fluid viscosity, as a function of volume fraction, with the same approach of the classical linear relationship introduced by Einstein [47]. These classical approaches underestimate experimental viscosities, but many similar correlations with variable degree volume fraction polynomials have been since proposed, as for instance the one by Chow [48]:

$$\eta_r = \frac{\eta_{nf}}{\eta_0} = 1 + \sum_{i=1}^{N} C_i \phi^i \tag{5}$$

where N represents the degree of the polynomial and C_i are the corresponding correlation coefficients. Eq. (5) trivially reduces to the

Fig. 5. Plot of thermal conductivity enhancement at 303.15 K of Co$_3$O$_4$/EG nanofluids as a function of the volume fraction. Experimental points: ($\bullet$); predicted values: (—) Maxwell Model; (— —) H–C Model and ($\cdots\cdots$) Turian Model.

Fig. 8. Viscosity increase enhancement as a function of volume fraction. (○) EG/Co$_3$O$_4$ nanofluids. (········) Prediction of Einstein equation; (———) Eq. (5) with $N = 1$; (—·—·—) Eq. (7), considering constant a_a/a ratio; (—) Eq. (7), considering variable a_a/a ratio.

Einstein [47] equation if $N = 1$ and $C_1 = 2.5$. Fig. 7 shows the underestimation of the viscosity enhancement yielded for Einstein relation, with departures increasing with concentration. The correlation with Eq. (5) was then considered, and if the value $N = 1$ is fixed, a C_1 value of 7.1 is obtained, producing average percent deviations of 0.8% (see also Fig. 8). Setting $N = 2$ in Eq. (5) does not bring much improvement to this correlation. Another alternative is the use of the following semi-empirical equation proposed to account for the viscosity of dispersions over wide concentration ranges, and introduced by Krieger and Dougherty [49]:

$$\eta_r = \frac{\eta_{nf}}{\eta_0} = \left(1 - \frac{\phi}{\phi_m}\right)^{-[\eta]\phi_m} \tag{6}$$

where ϕ_m is the maximum nanoparticle volume fraction, and $[\eta]$ is the intrinsic viscosity, which is agreed to be 2.5 for dispersions of equal sized hard spheres. In addition, if the suspended particles are assumed to form stable aggregates, its contribution to the total flow must be also computed. Keeping in mind these effects of variable packing fraction within the aggregate structure, an estimate for the viscosity enhancement can be expressed as [50]:

$$\eta_r = \left[1 - \frac{\phi}{0.605}\left(\frac{a_a}{a}\right)^{1.2}\right]^{-1.5125} \tag{7}$$

where a_a and a represent the estimated radius of aggregates and single particles. This theory points at the aggregation state of the suspended particles as the leading factor for the nanofluid viscosity enhancement. Newtonian behaviour has been proved in this case, and the viscosity enhancement depends on particle concentration but not of temperature, and as a first approach the radius of the aggregates has been considered concentration dependent. Then, the a_a/a ratio has been determined for each concentration, yielding results ranging between 1.9 and 2.3. This correlation is plotted also in Fig. 8, obtaining deviations in the same order of magnitude than experimental uncertainties, which evidences the ability of this model. Then, Eq. (7) was applied considering constant values for a_a/a, resulting in value of 2, and viscosity average percent deviations of 1.4%.

3.3. Density

The volumetric behaviour of the nanofluid samples studied were characterised by measurements of the experimental density for 1–5% in weight fraction, and a pressure range between 0.1 and 45 MPa at the temperatures of 283.15, 303.15 and 323.15 K.
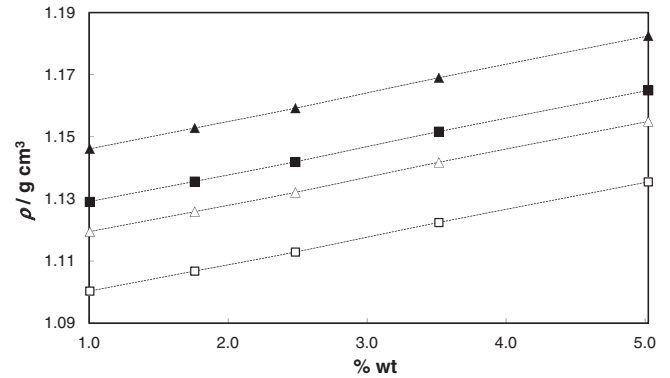
Fig. 9. Density (ρ) for Co$_3$O$_4$/EG nanofluids at different temperatures and pressures. Black symbols: 283.15 K; white symbols: 323.15 K; squares: 0.1 MPa and triangles: 45 MPa. The dotted line represents the correlation with Tammann–Tait equation.
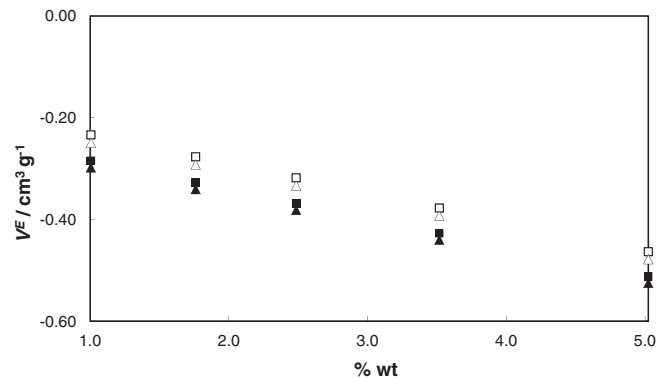
Fig. 10. Excess specific volume (V^E) for Co$_3$O$_4$/EG nanofluids at different temperatures and pressures. Black symbols: 283.15 K; white symbols: 323.15 K; squares: 0.1 MPa and triangles: 45 MPa.

The experimental results obtained are plotted in Fig. 9. The tendency found with pressure and temperature is in concordance with the standard behaviour of the base fluid, as ρ increases with pressure and decreases with temperature. The experimental density results were correlated by Tammann–Tait equation.

Making an analogy to a non-ideal fluid mixture the excess specific volume can be calculated, using in this case a mass basis:

$$V^E = \frac{1}{\rho_{nf}} - \sum_{i=1}^{n} \frac{w_i}{\rho_i} \tag{8}$$

where w refers to mass fraction, n is the number of mixture components, and nf stands for the nanofluid. Fig. 10 shows the V^E values as a function of volume fraction, ϕ, at 283.15 K and 323.15 K, and at two pressures, 0.1 MPa and 45 MPa. The values calculated from Eq. (8) do not correspond to an excess property from a thermodynamic point of view, as base fluid and nanoparticles are not in the same state. However, the procedure was employed previously to give an account of volume non additivity for these systems [30,51,52]. The volumetric deviation from ideal behaviour is significant, and deviations from ideality increase with nanoparticle concentration and pressure, and decrease when temperature increases. This trend might be attributed to the interface effects on the bulk fluid properties produced by the solid nanoparticle surface, or also to the nanoparticles interactions, so neglecting this type of interactions within a nanofluid is only a first order approximation.

4. Conclusions

Thermal conductivities and rheological behaviour of cobalt(II, III) oxide in ethylene glycol nanofluids have been determined experimentally as a function of volume concentration and temperature. Also, density as a function of these variables and pressure were measured. For thermal conductivity enhancements up to 27% at T = 323.15 K and 5.7% volume fraction were found.

The Newtonian nature of Co_3O_4/EG nanofluids for the concentration studied was demonstrated, and as expected viscosity increases with concentration and decreases with temperature. The Vogel–Tammann–Fulcher correlation equation was used to fit experimental viscosity, showing good agreement when applied to nanofluids. Concerning nanofluid viscosity representation, the method of Krieger and Dougherty, links the viscosity enhancement in a nanofluid only to its aggregation state produces fairly good results, so in this case the consideration of other possible variables affecting this transport property is not necessary.

The volumetric behaviour shows a significant contractive trend on mixing, which is affected by concentration, temperature and also by pressure, although the influence of this last variable is less important.

Conflict of interest

None declared.

Acknowledgements

References

[1] R. Prasher, D. Song, J. Wang, P. Phelan, Measurements of nanofluid viscosity and its implications for thermal applications, Appl. Phys. Lett. 89 (2006) 133108.

[2] J.L. Jiménez-Pérez, A. Cruz-Orea, J.F. Sánchez-Ramírez, F. Sánchez-Sinencio, L. Martínez-Pérez, G.A. López Muñoz, Thermal characterization of nanofluids with different solvents, Int. J. Thermophys. 30 (2009) 1227–1233.

[3] M.P. Beck, Y. Yuan, P. Warrier, A.S. Teja, The effect of particle size on the thermal conductivity of alumina nanofluids, J. Nanopart. Res. 11 (2009) 1129–1136.

[4] M.J. Pastoriza-Gallego, C. Casanova, R. Páramo, B. Barbés, J.L. Legido, M.M. Pineiro, A study on stability and thermophysical properties (density and viscosity) of Al_2O_3 in water nanofluid, J. Appl. Phys. 106 (2009) 064301.

[5] G. Paul, T. Pal, I. Manna, Thermo-physical property measurement of nano-gold dispersed water based nanofluids prepared by chemical precipitation technique, J. Colloid Interface Sci. 349 (2010) 434–437.

[6] M.P. Beck, Y. Yuan, P. Warrier, A.S. Teja, The thermal conductivity of alumina nanofluids in water, ethylene glycol, and ethylene glycol + water mixtures, J. Nanopart. Res. 12 (2010) 1469–1477.

[7] S.W. Lee, S.D. Park, I.C. Bang, J.H. Kim, Investigation of viscosity and thermal conductivity of SiC nanofluids for heat transfer applications, Int. J. Heat Mass Transfer 54 (2011) 433–438.

[8] I. Palabiyik, Z. Musina, S. Witharana, Y. Ding, Dispersion stability and thermal conductivity of propyleneglycol based nanofluids, J. Nanopart. Res. 13 (2011) 5049–5055.

[9] B. Ruan, A. Mm Jacobi, Ultrasonication effects on thermal and rheological properties of carbon nanotube suspensions, Nanoscale Res. Lett. 7 (2012) 127.

[10] J. Philip, P.D. Shima, Thermal properties of nanofluids, Adv. Colloid Interface Sci. 183 (184) (2012) 30–45.

[11] S.M.S. Murshed, K.C. Leong, C. Yang, Thermophysical and electrokinetic properties of nanofluids. A critical review, Appl. Therm. Eng. 28 (17/18) (2008) 2109–2125.

[12] E.V. Timofeeva, A.N. Gavrilov, J.M. Mccloskey, Y.V. Tolmachev, S. Sprunt, L.M. Lopatina, J.V. Selinger, Thermal conductivity and particle agglomeration in alumina nanofluids: experiment and theory, Phys. Rev. E 76 (6) (2007) 061203.

[13] J. Buongiorno et al., A benchmark study on the thermal conductivity of nanofluids, J. Appl. Phys. 106 (9) (2009) 094312.

[14] P.K. Namburu, D.P. Kulkarni, A. Dandekar, D.K. Das, Experimental investigation of viscosity and specific heat of silicon dioxide nanofluids, Micro Nano Lett. 2 (3) (2007) 67–71.

[15] H. Chen, Y. Ding, C. Tan, Rheological behaviour of nanofluids, New J. Phys. 9 (2007) 367.

[16] J. Chevalier, O. Tillement, F. Ayela, Rheological properties of nanofluids flowing through microchannels, Appl. Phys. Lett. 91 (23) (2007) 233103.

[17] H. Xie, L. Chen, Q. Wu, Measurements of the viscosity of suspensions (nanofluids) containing nanosized Al_2O_3 particles, High Temp.-High Press. 37 (2008) 127–135.

[18] H. Chen, Y. Ding, A. Lapkin, X. Fan, Rheological behaviour of ethylene glycol-titanate nanotube nanofluids, J. Nanopart. Res. 11 (6) (2009) 1513–1520.

[19] D.R. Heine, M.K. Petersen, G.S. Grest, Effect of particle shape and charge on bulk rheology of nanoparticle suspensions, J. Chem. Phys. 132 (18) (2010) 184509.

[20] M.J. Pastoriza-Gallego, L. Lugo, J.L. Legido, M.M. Piñeiro, Rheological non-Newtonian behaviour of ethylene glycol-based Fe_2O_3 nanofluids, Nanoscale Res. Lett. 6 (2011) 560.

[21] M.J. Pastoriza-Gallego, M.J. Pérez-Rodríguez, M. Gracia-Fernández, M.M. Piñeiro, Study of viscoelastic properties of magnetic nanofluids: an insight into their internal structure, Soft Matter. 9 (48) (2013) 11690–11698.

[22] R. Saidur, S.N. Kazi, M.S. Hossain, M.M. Rahman, H.A. Mohammed, A review on the performance of nanoparticles suspended with lubricating oils in refrigeration systems, Renew. Sustainable Energy Rev. 15 (2011) 310–323.

[23] H. Yoshikawa, K. Hayashida, Y. Kozuka, A. Horiguchi, K. Awaga, S. Bandow, S. Iijima, Preparation and magnetic properties of hollow nano-spheres of cobalt and cobalt oxide: drastic cooling-field effects on remnant magnetization of antiferromagnet, Appl. Phys. Lett. 85 (22) (2004) 5287–5289.

[24] S.A. Makhlouf, Magnetic properties of Co_3O_4 nanoparticles, J. Magn. Magn. Mater. 246 (2002) 184–190.

[25] S. Thota, A. Kumar, J. Kumar, Optical, electrical and magnetic properties of Co_3O_4 nanocrystallites obtained by thermal decomposition of sol–gel derived oxalates, Mater. Sci. Eng. B 164 (2009) 30–37.

[26] H.T. Zhu, J. Luo, J.K. Liang, G.H. Rao, J.B. Li, J.Y. Zhang, Z.M. Dub, Synthesis and magnetic properties of antiferromagnetic Co_3O_4 nanoparticles, Physica B 403 (2008) 3141–3145.

[27] D. Vickers, L.A. Archer, T. Floyd-Smith, Synthesis and characterization of cubic cobalt oxide nanocomposite fluids, Colloids Surf. A 348 (2009) 39–44.

[28] S.M. Hosseini, E. Ghasemi, A. Fazlali, D.E. Henneke, The effect of nanoparticle concentration on the rheological properties of paraffin-based Co_3O_4 ferrofluids, J. Nanopart. Res. 14 (2012) 858.

[29] H.S. Carslaw, J. Jc, Conduction of Heat in Solids, vol. 25, Oxford University Press, London, 1959.

[30] M.J. Pastoriza-Gallego, L. Lugo, J.L. Legido, M.M. Piñeiro, Enhancement of thermal conductivity and volumetric behavior of FexOy nanofluids, J. Appl. Phys. 110 (1) (2011) 014309.

[31] M.J. Pastoriza-Gallego, L. Lugo, J.L. Legido, M.M. Piñeiro, Thermal conductivity and viscosity measurements of ethylene glycol-based Al_2O_3 nanofluids, Nanoscale Res. Lett. 6 (1) (2011) 221.

[32] D. Cabaleiro, M.J. Pastoriza-Gallego, M.M. Piñeiro, J.L. Legido, L. Lugo, Thermophysical properties of (diphenyl ether + biphenyl) mixtures for their use as heat transfer fluids, J. Chem. Thermodyn. 50 (2012) 80–88.

[33] A. Mariano, M.J. Pastoriza-Gallego, L. Lugo, A. Camacho, S. Canzonieri, M.M. Piñeiro, Thermal conductivity, rheological behaviour and density of non-Newtonian ethylene glycol-based SnO_2 nanofluids, Fluid Phase Equilib. 337 (2013) 119–124.

[34] M.M. Piñeiro, D. Bessieres, J.M. Gacio, H. Saint-Guirons, J.L. Legido, Determination of high-pressure liquid density for *n*-perfluorohexane and *n*-perfluorononane, Fluid Phase Equilib. 220 (1) (2004) 127–136.

[35] M.M. Piñeiro, D. Bessieres, J.L. Legido, H. Saint-Guirons, PρT measurements of nonafluorobutyl methyl ether and nonafluorobutyl ethyl ether between 283.15 and 323.15 K at pressures up to 40 MPa, Int. J. Thermophys. 24 (5) (2003) 1265–1276.

[36] B. Lagourette, C. Boned, H. Saint-Guirons, P. Xans, H. Zhou, Densimeter calibration method versus temperature and pressure, Meas. Sci. Technol. 3 (1992) 699–703.

[37] B. Yang, Z.H. Han, Temperature-dependent thermal conductivity of nanorod-based nanofluids, Appl. Phys. Lett. 89 (2006) 083111.

[38] W. Duangthongsuk, S. Wongwises, Measurement of temperature-dependent thermal conductivity and viscosity of TiO_2–water nanofluids, Exp. Therm. Fluid Sci. 33 (2009) 706–714.

[39] D. Shima, J. Philip, B.R. Shima, Synthesis of aqueous and nonaqueous iron oxide nanofluids and study of temperature dependence on thermal conductivity and viscosity, J. Phys. Chem. C 114 (2010) 18825–18833.

[40] A.S. Teja, M.P. Beck, Y. Yuan, P. Warrier, The limiting behavior of the thermal conductivity of nanoparticles and nanofluids, J. App. Phys. 107 (2010) 114319.

[41] J.C. Maxwell, A Treatise on Electricity and Magnetism, Oxford University Press, London, 1892.

[42] R.L. Hamilton, O.K. Crosser, Thermal conductivity of heterogeneous two component systems, Ind. Eng. Chem. Fundam. 1 (3) (1962) 187–191.

[43] R.M. Turian, D.J. Sung, F.L. Hsu, Thermal conductivity of granular coals, coal-water mixtures and multi-solid/liquid suspensions, Fuel 70 (1991) 1157–1172.

[44] S.K. Das, S.U.S. Choi, W. Yu, T. Pradeep, Nanofluids: Science and Technology, Wiley, New York, 2008.

[45] P. Sahoo, H. Djieutedjeua, P.F.P. Poudeu, Co_3O_4 nanostructures: the effect of synthesis conditions on particles size, magnetism and transport properties, J. Mater. Chem. A 1 (2013) 15022–15030.

[46] M.J.P. Comuñas, J.P. Bazile, L. Lugo, A. Baylaucq, J. Fernández, C. Boned, Influence of the molecular structure on the volumetric properties and viscosities of dialkyl adipates (dimethyl, diethyl and diisobutyl adipates), J. Chem. Eng. Data 55 (9) (2010) 3697–3703.

[47] A. Einstein, On the movement of small particles suspended in stationary liquids required by the molecular-kinetic theory of heat, Ann. Phys. 17 (1905) 549–560.

[48] T.S. Chow, Viscosities of concentrated dispersions, Phys. Rev. E 48 (1993) 1977–1983.

[49] I.M. Krieger, T.J. Dougherty, A mechanism for non-Newtonian flow in suspensions of rigid spheres, Trans. Soc. Rheol. 3 (1959) 137–152.

[50] H. Chen, Y. Ding, C. Tan, Rheological behaviour of nanofluids, New J. Phys. 9 (367) (2007) 1–24.

[51] C. Wei, Z. Nan, X. Wang, Z. Tan, Investigation on thermodynamic properties of a water-based hematite nanofluid, J. Chem. Eng. Data 55 (7) (2010) 2524–2528.

[52] M.J. Pastoriza-Gallego, C. Casanova, J.L. Legido, M.M. Piñeiro, CuO in water nanofluid: influence of particle size and polydispersity on volumetric behaviour and viscosity, Fluid Phase Equilib. 300 (2011) 188–196.